national accelerator laboratory

TM-546
6029

FEASIBILITY STUDY ON THE DESIGNS OF SHORT LIVED BEAMS IN THE PROTON CENTRAL EXPERIMENTAL AREA

D. P. Eartly

April 2, 1975

FEASIBILITY STUDY ON THE DESIGNS OF SHORT LIVED BEAMS IN THE PROTON CENTRAL EXPERIMENTAL AREA

The Proton Experimental Area consists of three separate proton beams and subsequent enclosures resulting from the split of the primary proton beam in Enclosure H of the Switchyard, as shown in the layout figure.

The Proton East Area contains Experiments 87A, 358, 25 and 300. Experiments 87A and 358 utilize a wide band photon beam facility, and Experiment 25 utilizes an electron beam - tagged photon facility, while E-300 is a large angle spectrometer.

The Proton Central Area houses Experiments 288 and 48, consisting of a two-arm lepton spectrometer and a muon polarization spectrometer, respectively. The Proton West Area contains Experiments 95, 284, and 177, consisting of thin target widely variable angle charged particle and photon spectrometers in an upstream hall, followed by the wide angle scattering two-arm spectrometer of Experiment 177.

The Proton East Area consists of a relatively long concrete tunnel and enclosure for an upstream focussing, beam switching and targeting-dump system for the facility photon and electron-tagged photon beam branches; followed by a sheet pile pit housing the beams and Experiment 300. The experimental area for E-87A is a subsequent concrete enclosure, and for E-25, the tagging laboratory building.

Historically, the Proton Central Area came to consist of a constraining concrete tunnel and enclosure for an upstream focussing and targeting-dump system, followed by a sheet pile experimental area. A short (22 ft.) shielded target-dump system was developed in the enclosure for Experiment 70, within the boundary conditions.

Futuristically, we look to the possible evolution of the area. Considering the layout, the area could be used to advantage as a high flux short lived beam facility if the existing target system could accommodate the requirements of these beams. See Figure 1.

In this report, designs for neutral and negatively charged short lived beams, which are consistent with the target system, are taken up in detail. It appears that the area could provide a unique facility of these beams.

DPE:al

I. A Preliminary Design Report on Short Lived Neutral Beams for the Proton Central Experimental Area

In a detailed analysis, it appears quite possible to establish a unique short lived beam facility in the Proton Central Area utilizing the present target box system in conjunction with a sweeping collimator similar to that setup in the M2 beam (E2 B10) of the Meson Area.

A well focused 400 GeV/c beam of up to 2 x 10^{12}/pulse can be accommodated by the 1½ mm tungsten target and the tungsten beam dump, 3m downstream. LINDA calculations indicate that horizontal sweeping fields of 26Kg ($\int$ Bdl = 462 Kg ft.) can be achieved by magnets consistent with the target system geometry in the Target-Dump-Defining Collimator region of the 1 μstr. beam.

A subsequent 6m vertical field sweeping collimator like E2 B10 provides an additional sweeping ($\int$ Bdl $\sim$ 360 Kg ft.), hadron shielding corresponding to the forward 10^{-10} star density contour, and forward muon depletion.

Utilizing a displacement and pitching of the proton beam, production angles from 0 to 9 mr can be achieved. The beam length is 12.5 m.

The proposed target box system for neutral short lived beams is schematically illustrated in Figure 2. It consists of a necessary backshield, a beam locating SWIC, an 8 cm long W-2% ThO target at the entrance of the first of two identical sweeping magnets H_1, H_2 which surround a pre-collimator sweeping region, and a defining collimator - beam dump region respectively. H_2 is followed by a necessary personnel shield. A detail of the collimator - dump regions has been developed.

The measured proton beam emittance (typical) is 1.5 mmmr (Horizontal) x 0.7 mmmr (Vertical). A double focus of 1 mm x 1 mm is achievable. Thus, a 1½ mm dia target, which is significantly smaller than the defining collimator, is satisfactory. To enable the W target to sustain beam intensities which are acceptable to the dump (≤ 2.10^{12}/pulse), the target will be suspended in a subcooled water bath as illustrated in Figure 3. In this configuration, the maximum target temperature is determined by the pulsed temperature jump $\Delta T_p \lesssim 350^oC/10^{12}$ (0.7 sec. eff. spill) and is given by $T_m \simeq T_{water} + \Delta T_p$ since the time constants are very short. The maximum radial compressive stress Σ_r is 77.1 kpsi/10^{12}, well within elastic limits (Figure 4). The peak power absorption is 128 w/10^{12} (0.7 sec. eff. spill) corresponding to a peak instantaneous heat transfer $\dot{Q}$ = 34 w/cm^2 within the limits of laminar flow non-boiling heat transfer. While this configuration results in a high irradiation of the small amount surrounding water in the closed loop water system, experience with Experiment 100 W Targets in Proton East indicates this scheme is necessary.

Beam steering on the target will be monitored with a radiation resistant SWIC* (Mycalex) at the target and effected by two upstream steering dipoles. The modular assembly of the target allows for quick exchange or replacement.

As the target will reach activation levels of 5 - 10R**, the upstream region must be shielded for personnel occupancy. Using high purity $CaCO_3$, residual γ attenuation of x 100 requires 30 cm of absorber (Figure 5).

To minimize the distance between the target and an "out of sight" beam dump, the sweeping field - collimator system incorporates a number of special features. First of all, the residual beam is deflected vertically downwards; taking advantage of the smaller vertical emmittance in separating the protons from the neutral beam, and in pointing the forward background downwards away from downstream detectors. Secondly, given the geometrical and power limitations (cooling system 158 KW and 50 gpm, present power supplies, etc.), maximum field (26 Kg) identical sweeping magnets were designed which satisfy these requirements. The characteristics of H_1, H_2 are given in Table I, a section view in Figure 6, and the field distribution in Figure 7. These magnets provide 462 Kg ft. of sweeping. Finally, the system includes tapered collimators with the neutral beam defining collimator focused upstream of the target by 16".

For the beam configuration given by Figure 1, the proton separation vs. distance from the target is given in Table II. Since Electromagnetic effects in a dump build up in $6\lambda_R$ (≃ 1" in tungsten), one must allow 1 - $2\lambda_R$ (3.6 - 7.2 mm) transversely between the dump point and the

* Pin Mounted/Located
** As Measured for Experiment 100 Targets

neutral beam apeture for 0 mr production. Coupled with activation limitations at the downstream end, a distance of 3 m from the target (10 cm inside the H_2 core) seems workable for the dump position, providing 2.6 m of dump within the shielded target system. Taking this to be all tungsten (1 cm x 260 cm x 5 cm) and accounting for the ratio of absorption lengths (0.606), Figure 8 extrapolated to 400 GeV/c indicates that this corresponds to the $\leq 10^{-4}$ star density contour or a very low residual activation.* If necessary, a partial substitution with copper would be permissible.

Thus the core of H_1 defines the pre-collimator region, while the core of H_2 corresponds to the neutral beam defining collimator and beam dump region (Figure 2). As illustrated, the pre-collimator is vertically large (10 mm at the target) and tapered open (42 mm at the downstream end of H_1) to accomodate neutral beam production angles up to 9 mr; achieved by pitching the proton beam down at that angle through the target. Vertically, the neutral beam edge of the pre-collimator pitches in from 5 mm at the target to a constant 2.5 mm at $\geq$ 1 m. Horizontally, the collimator tapers from 10 mm at the target to 7 mm (required clearance for the proton beam) at the downstream end. The value of these tapers (against diffraction scattering) is an open question. A constant width of ± 5 mm (horizontally) and 5 mm (vertically) on the neutral beam side may be almost as good.

The core of H_2 contains a defining collimator for the 1 μstr neutral beam (± 1.7 mm x ± 1.7 mm) at the upstream end, tapered to (± 3 mm x ± 3 mm) at the downstream end. This apeture (3 sides) is cut into a single piece of copper wedged between the pole tips of H_2, registered to a return leg of the magnet, and water cooled to prevent distortion induced by heating from secondary particle absorption (Figure 9). The magnet coils will be isolated from the collimator using crystalline mica or ceramic insulation. Downstream of the beginning of the dump, the collimator contains a $8\lambda_R\gamma$ converter.

To accommodate production angles from 0 - 9 mr, the beam dump must accept a vertical proton beam displacement of -5 mm to -37 mm. Thus, the water vessel and upper edge of the dump must make up the remaining edge of the collimator. The dump must fill a region (1 cm x 260 cm x 5 cm).

To use a heavy metal, one must consider tungsten in some form on the basis of thermal conductivity and tensile strength. However, the peak energy deposition occurs in the electromagnetic shower region (5 - 35 λ_R) and the very short radiation length results in high energy deposition densities (Figures 10 and 11). In a simplest approach on could consider a tungsten rectangle cooled only by a water path along the bottom edge. Appendix I outlines the dump calculations which are summarized in Table II. For 10^{12}

* Iron Equivalent. The activation of F_e and W are equal on the long term. W is 2 times as active on the short term. (Barbier)

protons, only one tungsten sinter Mallory Gyromet 1100 (Figure 12) has an Ultimate tensile strength exceeding the compressive stress; but the characteristics of such sinters vary from sample to sample. More critically, the peak heat transfer rate at the water boundary is 1100 watts/cm^2; a dangerous upper bound for boiling heat transfer to a well mixed, subcooled bulk water path. This scheme is simply too limiting.

To accommodate intensities like 10^{12} the physical configuration must increase the surface area and reduce the time constants for heat transfer without making the dump "transparent". One possible configuration consists of a vertical slab cooled on one or both faces. However, to maintain a cold bulk fluid volume to collapse the boundary vapor layer for satisfactory boiling heat transfer, too much of the small section area is taken up by water. This results in high irradiation of the water and a substantial transparency of the front of the dump. A more complex but satisfactory scheme is shown in Figure 13. The front 30 cm of the dump consists of a stack of W - 2% ThO rods in a water bath. For a reasonable quantized set of production angles, the beam profile strikes the centers of the rods keeping the water $1\lambda_R$ away from the core of the beam. The cooling time constants are very short and the surface area is increased so as one can observe from Table III., the maximum mean temperature T_M equals the pulsed temperature jump plus the vapor barrier temperature jump and the maximum stress is within the elastic limit up to $\lesssim 2.10^{12}$ pro/pulse. For 2.10^{12} pro/pulse, the instantaneous boiling heat transfer rate reaches a high value $\sim$ 900 w/cm^2. However, this configuration provides a bulk fluid volume and high drag conditions.

The upper (collimator) edge consists of a continuous strip of tungsten.

To decrease the transparency, the next 31 cm of the dump consists of a water path transition guide (spider) and a stack of tantulum hexagons displaced with respect to the W - 2% ThO rods so as to mask the preceeding water paths. In this region, the heating is decreased and the heat transfer remains adequate for the configuration.

In the remainder of the dump, the use of one edge cooled vertically staggered tungsten slabs is acceptable with the water path alternating between the upper and lower edges. With smoothly tapered corners (well beveled) the turbulence should be sufficiently limited. Again the top edge of this part of the dump would consist of a continuous piece of tungsten through all sections. With this three stage dump, the transparency is minimized. The dump vessel would be constrained and shielded by copper wedges between the H_2 poles and coils. The shielding underneath would consist of a cooled copper bar insulated from the coils with mica or ceramic. With a minimum of 2.6 m Fe equivalent shielding, downstream utility leads should be accessable behind a 30 cm $CaCO_3$ absorber.

The two downstream target system drawers on either side of the H_2 magnet would consist of low carbon iron shields magnetized with Helmholtz coils (500 AT/m) with a horizontal field $\underline{B}$ = 14 Kg to deflect forward muons.

To provide additional sweeping of the neutral beam and hadron shielding adequate for detectors just downstream, the system would utilize a massive vertical field sweeping collimator like E2 B10 just downstream of the target system. Dimensions like $\pm$ 3 feet vertically, $\pm$ 5 feet horizontally, and 18 feet longitudinally with a 3 foot coil window well match the requirements for a shielding plug (10^{-10} star density contour at 400 GeV/c). The sweeping field in the forward region is perpendicular to that of the target system magnets, so forward muons would be depleted. With coils like those in E2 B10 and a copper collimator gap of 0.75, large sweeping fields ((14.6 Kg) $\int BdL$ = 265 Kg ft.) can be achieved at 1100A, for the magnet in series with the target system magnets on a power supply available in the Proton Central area. Slow neutrons can be thermalized and absorbed at the end of the shield-collimator.

Predictions on the yields of particles in the beam have been obtained from the model of Hagedorn and Ranft as given by SPUKJ on hydrogen in FN-216 (400 GeV/c); with some modifications (see Figure 14). The Λ^o production has been taken as given. Using the cross section data (24.5 GeV/c) pp $\rightarrow \Sigma^-/(\Sigma^0,\Lambda^0)$ in CERN/HERA 70 - 2 of Bartke et. al. and extrapolated (to 400 GeV/c) values of $d^2N/d\Omega dp$ (Σ^-) of P - 353, one obtains values of $\frac{d^2N}{d\Omega dp}$ $(\Sigma^0,\Lambda^0) \sim \frac{1}{2}$ of the Hagedorn - Ranft model. Using the BNL data on Ξ^-/Σ^- vs ($P_{LX}/P_{LX\ MAX} = \alpha$) one could project Ξ^0/Λ^0 ratios of 1/20 $\rightarrow$ 1/100 as $\alpha \rightarrow 0.8$. To estimate Ξ^0, we apply a factor x 1/100 to the SPUKJ yield curve for Ξ corresponding to a factor of $\sim$ 1/200 Λ^0. This is an underestimate. If one applies the Ξ^-/Σ^- ratios per P - 353, a substantially higher Ξ^0 curve is obtained. All these are shown in Figure 15.

In conjunction with the design and analysis of short lived neutral beams, we attempted to consider the possibility of a common facility for both the neutral and charged beams. Maintaining the constraints that the charged beam should end up in the horizontal plane and be tunable over a reasonable momentum range ($\alpha = P_{Y^-}/P_{Y^-MAX} = 0.5 \rightarrow 1.0$), one arrives at the conclusion that this interferes with small production angles for neutral beams. Providing a reasonable ($\int BdL$ = 230 - 460 Kg ft.) sweeping field over the negative beam channel (11 mr deflection for P_{Y^-}) requires this very large pitch angle for the external proton beam; making the displacement-pitch (> 67 mm) tune of the external proton beam more difficult, power consuming and questionable than that required for large production angle neutral beams. This also results in the coincidence of the negative beam channel and the proton beam at the dump for 0^{O} production neutral beams. Considering this proton - neutral beam separation and the dump configuration, the negative beam cannot fit in between. An even larger pitch angle, if at all possible, results in $\alpha < 1.0$ for the negative beam. Thus, one considers independent exchangeable target system facilities and a different scheme.

To keep the negative beam in the horizontal plane and to avoid the power demand and manipulation of the external proton beam, we propose an alternate, interchangeable target system essentially like that for the neutral beam: except that it is now rotated from the vertical to the horizontal plane; i.e., the proton and negative beams are now dispersed horizontally.

The external proton beam steering and targeting would be identical to the 0 mr neutral beam system. Small production angles could be achieved with a magnet immediately in front of the target, now provided for Experiment 48, and the upstream steering magnets. We consider a tunable momentum range of 160 - 380 GeV/c ($\alpha_{\Sigma} \sim \frac{1}{2}$ to 1) for the negative beam at a constant total bend angle of 11 mr in the target system. Again, a dump at 3 meters from the target would appear to be the best situation.

The separations of the beam from the protons for various α is given in Table III. For $\alpha \sim \frac{1}{2}$, the minimum separation is comparable to the neutral beam case; however, the sweeping field is only half of the latter case.

Here the proton beam position has a more limited range in comparison to the variable production angle neutral beam; even if a small variation in production angle is allowed. Thus, one might consider a different beam dump configuration in trying to limit the irradiation of the closed loop water. However, face cooling configurations result in higher irradiation while edge cooling results in too long of time constants. Again the rod configuration (at least two rods) seems best. Consequently, a dump identical to that for the neutral beam appears appropriate.

The core of H_1 again defines a pre-collimator region. Vertically, the linear pre-collimator tapers from 9 mm at the target to 6 mm at the downstream end. (See Table IV). Horizontally, the linear pre-collimator tapers from 9 mm at the target to ± 12 mm (about the incident beam line).

The two beam profiles (P^+ and Y^-) just remain in the good field region (B_o, B_o - 2%) of the H_1 magnet.

To maintain the high sweeping field for the negative short lived beam in the H_2 defining collimator region, this magnet would be offset (assymmetric) on the negative beam side. The loss of field in the proton beam dump region should not significantly affect the spectrum of secondaries escaping the dump. A high field is maintained on the negative beam side of the dump.

The negative beam defining collimator in H_2 (beginning 10 cm inside the core) would consist of a tapered curved channel with an upstream apeture of 3.4 mm x 3.4 mm (broached for 15 cm) and a downstream apeture 6 mm x 6 mm corresponding to a 1 μstr solid angle.

Following the target system the sweeping collimator, as described in the neutral beam system, would contain a tapered, curved shadow collimator for the negative beam with apetures to match the defining collimator acceptance. The bend angle through this collimator would be 8.6 mr.

The large solid angle acceptance (± 0.5 mr, ± 0.5 mr) of the defining and shadow collimators results in a large momentum acceptance of the beam ($\Delta\theta$ = ± 1.67 mr* for θ_B = 19.6 mr) of $\frac{\Delta P}{P}$ (PW) = 17%.

Using two sets of two X, two Y staggered 1 mm PWC's spaced at 1 m; the momentum- angle correlation would allow a momentum measurement $\Delta P/P$ = ± 3%, with the uncertainty dominated by the production angle uncertainty.

By inserting a smaller collimator at the upstream end of the sweeping collimator, the momentum and/or angle acceptance can be reduced as desired.

Predictions on the yields of particles in the beam have been obtained in the following way. The π^- yield is taken from FN-216 (400 GeV/c) for a Pb target, obtained from the model of Hagedorn and Ranft as given by the Program SPUKJ. The Σ^- production has been obtained from SPUKJ using the Σ^+ curves with the ratio ($\Sigma^-/\Sigma^+ = \frac{1}{4}$) given by the BNL bubble chamber data in CERN/HERA 70 - 2 of Bartke et. al., finally modified by a factor of two to agree with P-353. The Ξ^- yields were derived from the Σ^- yields using the BNL yield ratio curves of P-353. Finally, the Ω^- yield was estimated from the Ξ^- yields assuming the ratio (Ω^-/Ξ^-) = (Ξ^-/Σ^-). These are shown in Figures 16 and 17.

* Assuming that both the defining and shadow collimators delimit the beam rays.

TABLE I.

PROTON LAB SWEEPING MAGNET - H1, H2

Field Strength	26kG
Magnet Length	106 - 108 in.*
Magnet Gap	.400 in.
Coil Aperture	.800 in.
Field Aperture	
Field Quality	± 1 per cent
Coil Turns	48
Copper Conductor Cross Section	.460 in. x .460 in.
Water Cooling Hole Diameter	.230 in.
Conductor Corner Radius	.0625 in.
Conductor Current	1,000 A
Magnet Inductance	.012 Hy
Coil Resistance	∿ .0522 Ω
Voltage Drop	≃ 52 v
Power	≃ 52 KW
Cooling Water Pressure	200 psi
Number of Water Paths	6
Water Flow	8.2 GPM
Temperature Rise	24.3°C
Outside Dimensions	12 in. x 12 in.
Iron Weight	3,800 lbs.
Copper Weight	600 lbs.

* Note: Pole ends must be tapered inwards at each end of the magnet to limit saturation. Taper should be comparable to the pole taper itself (∿ 1").

Note: This data on the magnets has been supplied by S. Snowden using LINDA calculations.

TABLE II. (A)

SEPARATION OF PROTON AND NEUTRAL BEAMS

Distance From Target	X_p (FW)	Y_p (FW)	Sagitta	Beam (FW) Edge* Displacement from Neutral Beam	1 μst = ΔΩ ΔX, ΔY (H. W.) Dimensions of Neutral Beam
0	1 mm	1 mm	0 mm	0 mm	0.20 mm
1 m	2.5	1.7	0.97	-0.58	0.70 mm
2 m	4.0	2.4	3.89	1.49	1.20
3 m	5.5	3.1	∼ 8.71 mm	5.46	1.70
4 m	7.0	3.8	14.97	10.37	2.20
5 m	8.5	4.5	23.14	18.19	2.70

TABLE II. (B)

Beam Dump Models, Parameters, and Characteristics (3 m from Target)

A. Edge Cooled Slab

$\frac{(1 + X_B Y_B)^{1/2}}{\lambda_R 2}$	Z (cm)	τ_{min} (sec)	$\Delta T/_{PUL}$ (^oC)	$T_{MAX} - T_o$ (^oC)	Q_{peak} (W/cm^2)	Σ_r	UTS (T_{MAX})
1.52	5	18.2	$167^o/10^{12}$ pro	$167^o/0.32 = 522^o$	1140	119 kpsi	125 kpsi Gyromet 1100

B. Stacked Rods

	R (cm)	τ_{min} (sec)					
1.52	0.5	0.08	$167^o/10^{12}$ pro	168^o (Add + 30^oC Vapor Barrier T Jump)	435	44kpsi	98kpsi W - 2%ThO (200^oC) 76kpsi (350^oC)

* Assumes all the beam is in 2FW phase space.

TABLE III.

SEPARATION OF THE NEGATIVE SHORT LIVED (1 μstr, ΔX (HW) = 1.7 mm)

AND PROTON BEAMS (X_p (FW) = 5.5 mm) at 3m FROM THE TARGET

α	P_{Y^-} (GeV/c)	Proton Sagitta (S_p)	Separation of Beams $R = (S_{Y^-} - \Delta X_{H^-} + S_p - X_p)$
0.5	∿ 190	4.35 mm	6.22 mm
0.6	228	5.22	7.08
0.7	266	6.10	7.96
0.8	304	6.97	8.83
0.9	342	7.84	9.70
1.0	∿ 380	8.71	10.57

Negative Beam Sagitta $S_{Y^-} \equiv 9.06$ mm: Note that R includes a proton beam size (2*FW) profile, as in the case of the neutral beam, to include essentially all the flux.

TABLE IV.

COLLIMATOR DIMENSIONS

A. Pre-Collimator

	VERTICAL			HORIZONTAL	
	Upstream	Downstream	Downstream Beam Dims	Upstream	Downstream
A. Pre-Collimator	9 mm	6 mm	(P^+) 3.1 mm FW (Y^-) 3.4 mm FW	9 mm	± 12 mm
B. Defining Collimator (curved)	3.4mm	6 mm		3.4 mm	6 mm

APPENDIX I.

Beam Dump Considerations

Model: Edge Cooled Slab

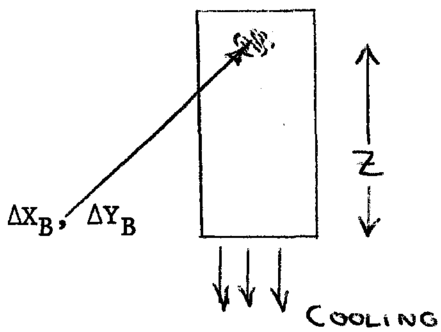

Tungsten Constants:

$1.6 * 10^{-10}$ joules/Gev
$\rho C_W = 2.58$ w sec/cm $^3/^oC$
$\tau_p = 7.0$ sec^{-1}

$(\delta E/\delta V)_{MAX} = 4.1$ GeV/cm^3/pro
$\rho C = 2.58$ watt sec/cm^3 ^oC
$k = 1.43$ watt/cm^2 ^oC

Model: Perimeter Cooled Rod

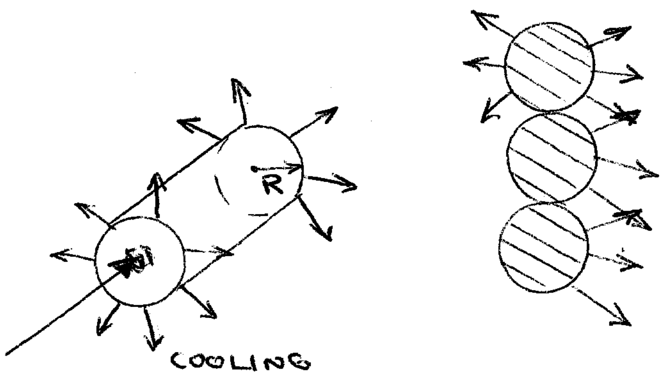

Pulse Temperature Jump

$$\frac{\Delta T\ (^oC)}{\text{pulse}} \simeq \frac{(\delta E/\delta V)_{MAX} * N_{pro}}{\rho C \left(1 + \frac{\Delta X_B\ \Delta Y_B}{\lambda_R^2}\right)^{1/2}}$$

Minimum Time Constant

$$\tau_m = \frac{4\rho C}{\pi^2 k} Z^2 = 0.73Z^2\ (\text{sec})$$

Maximum Mean Temperature

$$T_m - T_o = \Delta T/1 - e^{-\tau_p/\tau_m}$$

T_o = bulk cooling medium temperature

τm = minimum time constant

τp = spill rep. rate

Maximum Radial Stress

$$\Sigma_r = \alpha\varepsilon\Delta T = 220\ \text{psi}/^oC * \Delta T\ (^oC)$$

Minimum Time Constant

$$\tau m = \frac{\rho Cp}{k\xi_1^2} R^2 = 0.312\ R^2$$

ξ_1 = first zero of Bessel Function of ϕ
= 2.4048

Heat Transfer Rates (Radial Flow Only)

$$Q(Z) = \frac{\int P\ (r,z)\ rdr}{\text{Area of Cooling Surface}}$$

APPENDIX II.

Special Considerations on the Target System

For the magnets H_1 and H_2 there are a number of special considerations resulting from their location and function in the neutral beam system. Historical problems with ceramic insulations can be avoided through the implementation of mechanical sweged connections on the ends. This would allow removal of the water manifold and isolated replacement of one ceramic. By fanning these insulators and the manifold into the shielding plugs at the ends of the drawers, they can be readily serviced without removing the drawers or excessively exposing personnel. Power and utility connections (excepting the beam dump) would all be at these exposed ends.

Because of the very high irradiation of the magnet coils, it would be desirable to utilize a very radiation resistant insulation and bonding system. However, to date, we have not developed an adequate ceramic insulation scheme for coils. The use of mineral insulated coils like those at LAMPF (described in LA-5306-MS) is prohibitive on the basis of current density and power requirements. At present, the best scheme involves loaded epoxy vacuum impregnated coils with additional radiation resistant ground insulation (in the coil window, against collimators etc.,) provided by crystalline mica sheets or ceramic flame spray coatings on the mechanical parts. An integral modular target assembly has been described. With mechanical water connections, these can be quickly removed and replaced.

APPENDIX III.

Some Cost Estimates on the Target Box System

<u>Shields and Mounts</u>

\$ 0.50K	= \$0.50K	

<u>Magnets</u> (H_1 and H_2)

Cores \$4.8K each with buss, fittings, etc.	= 9.6 K	
Coils - copper \$0.90K each	= 1.8 K	Booster
(winding and Potting) \$10.0K total (12 pancakes)	= 10.0 K	Conductor

Appendix III. (cont'd.)

Collimators

H_1 pre-collimator (material and machining)	= $ 0.7 K
H_2 defining collimator	= 0.4 K
Tungsten Beam Dump	
(Vessel)	= 0.4K
(Tungsten Slabs)	= 0.5K
(Tantalum Hexes)	= 0.4K
(W - 2% ThO Rods)	= 0.1K
Water path matrix, guides, etc.	= 0.3K
Insulation, special materials, etc.	= 0.5K

Side Shielding Drawers

machining of reject billets (2) for coil winding and cooling	= 1.25K
	$25.5 K
Additional 45 Ton (15 BKW) Refrigerator	$20.0 K

DE:clc

16

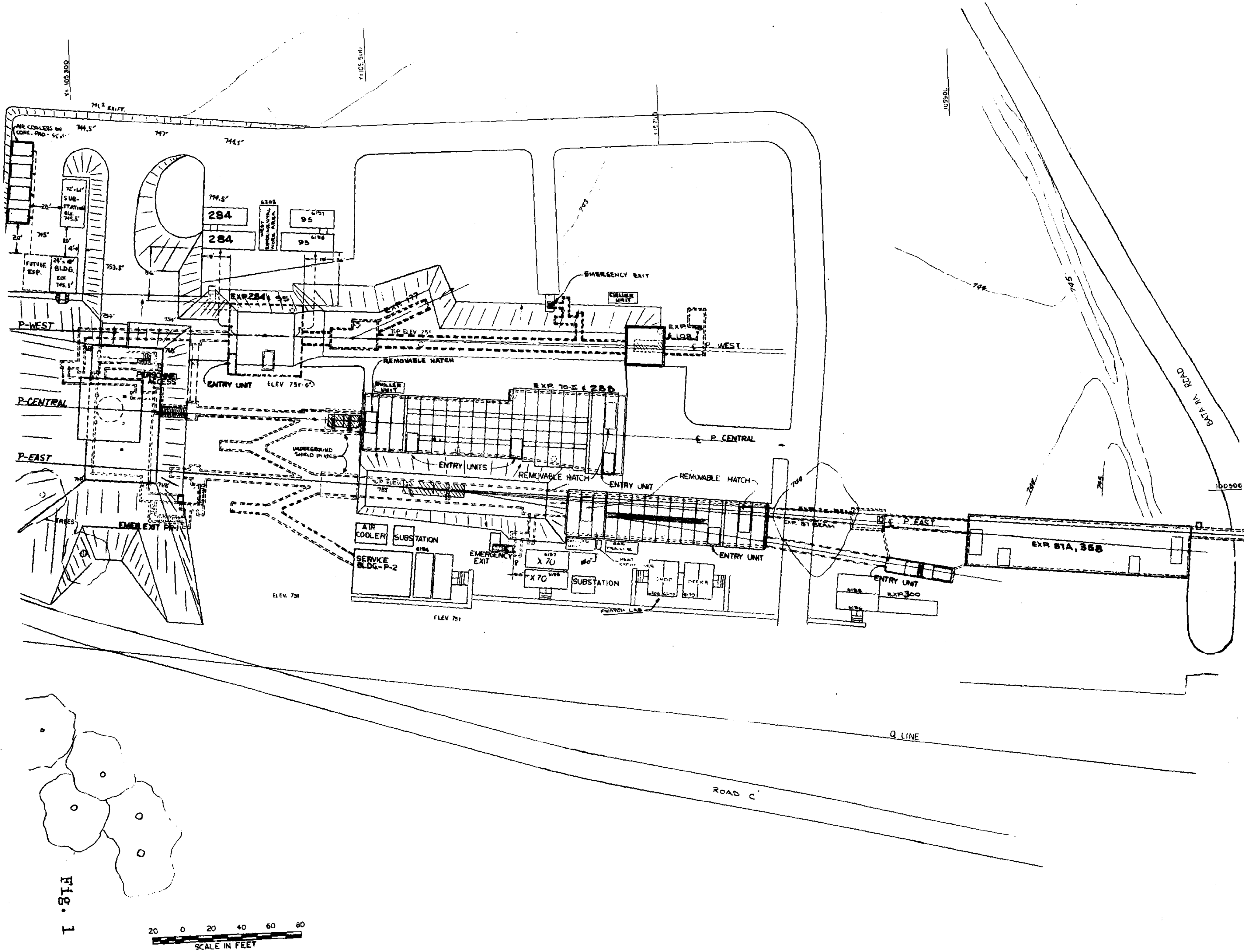

Fig. 1

TM-546

PROTON CENTRAL SHORT LIVED NEUTRAL BEAM TARGET SYSTEM

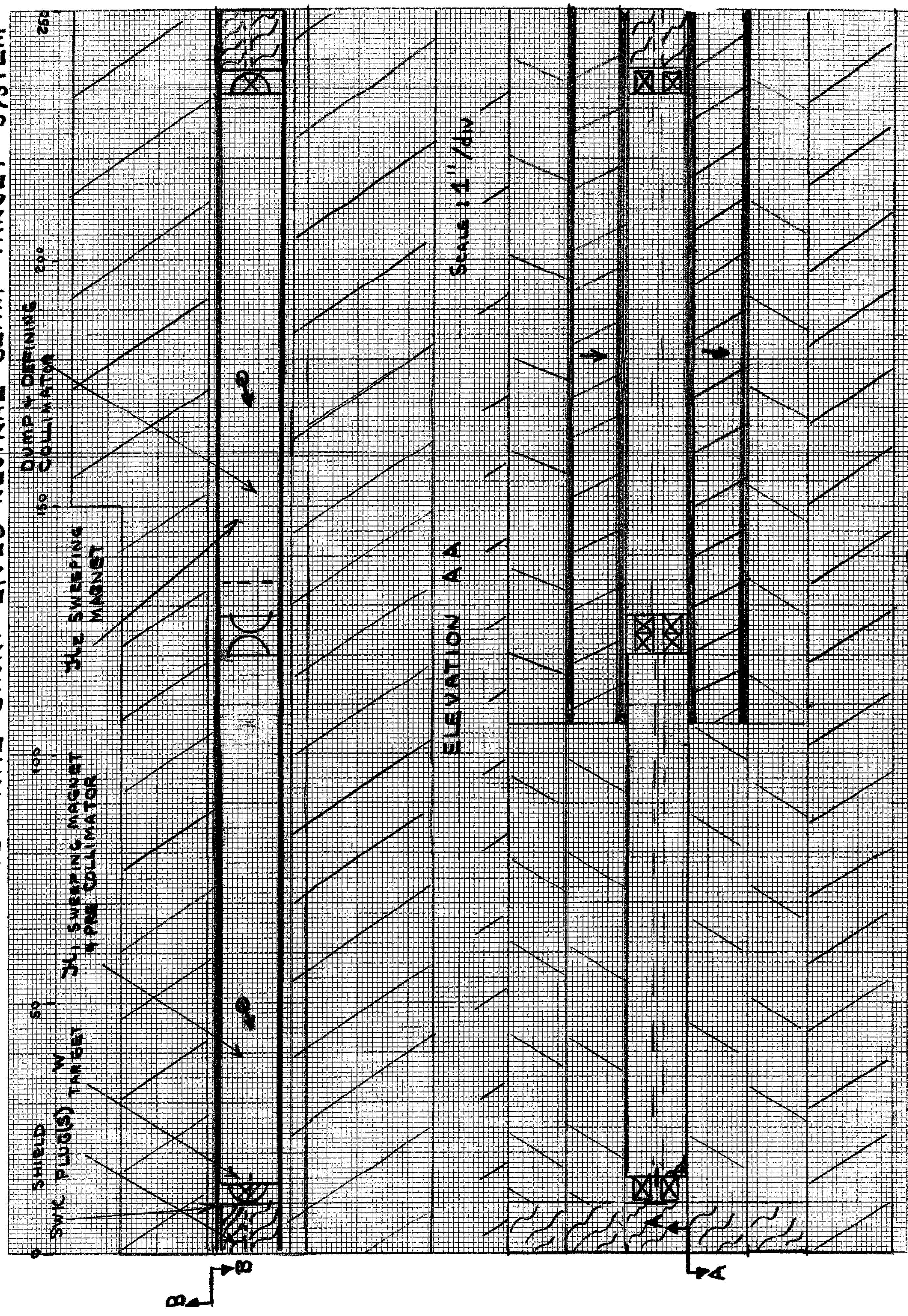

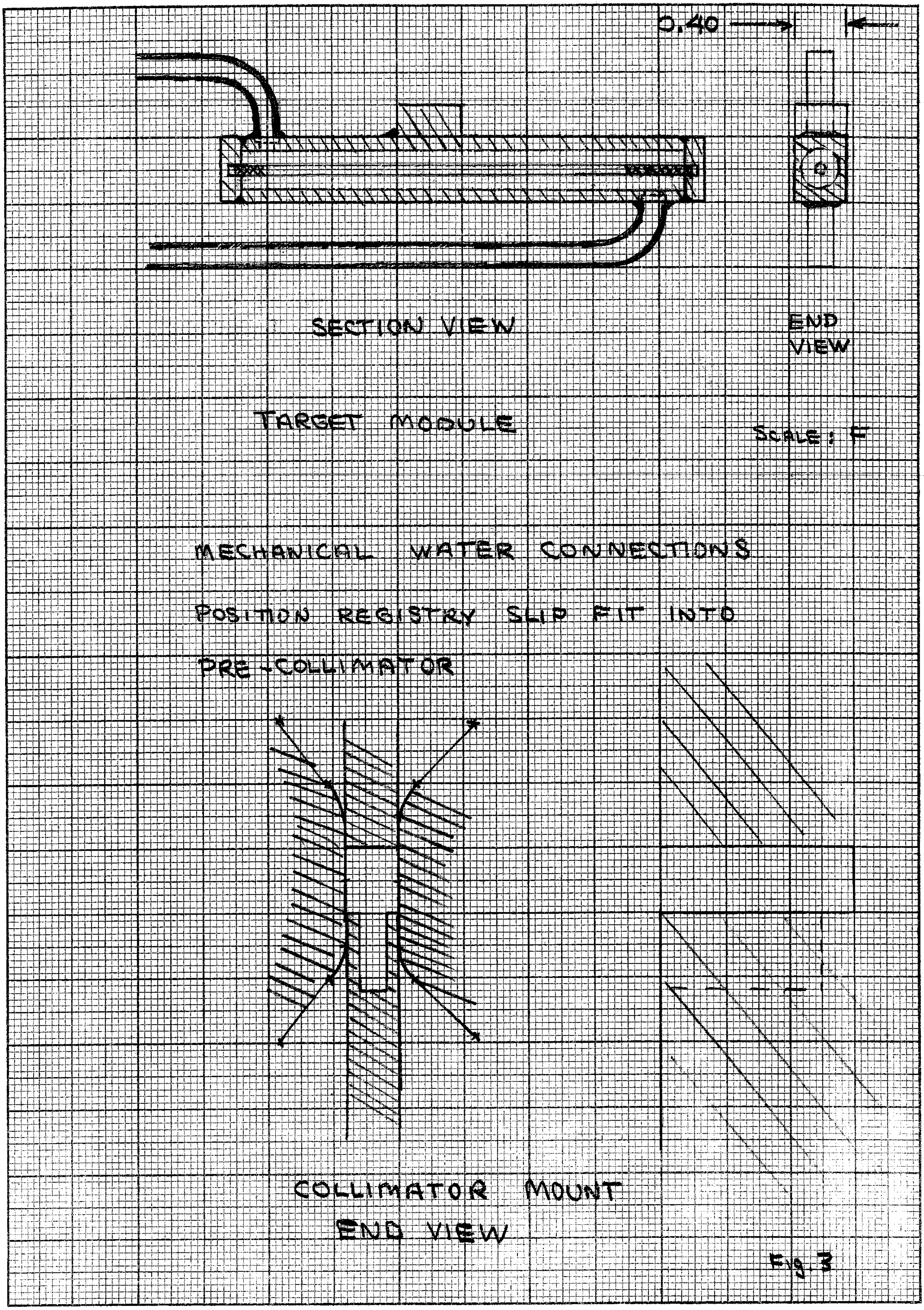
0.40
SECTION VIEW
END VIEW
TARGET MODULE
SCALE: F
MECHANICAL WATER CONNECTIONS
POSITION REGISTRY SLIP FIT INTO
PRE-COLLIMATOR
COLLIMATOR MOUNT
END VIEW

Fig. 3

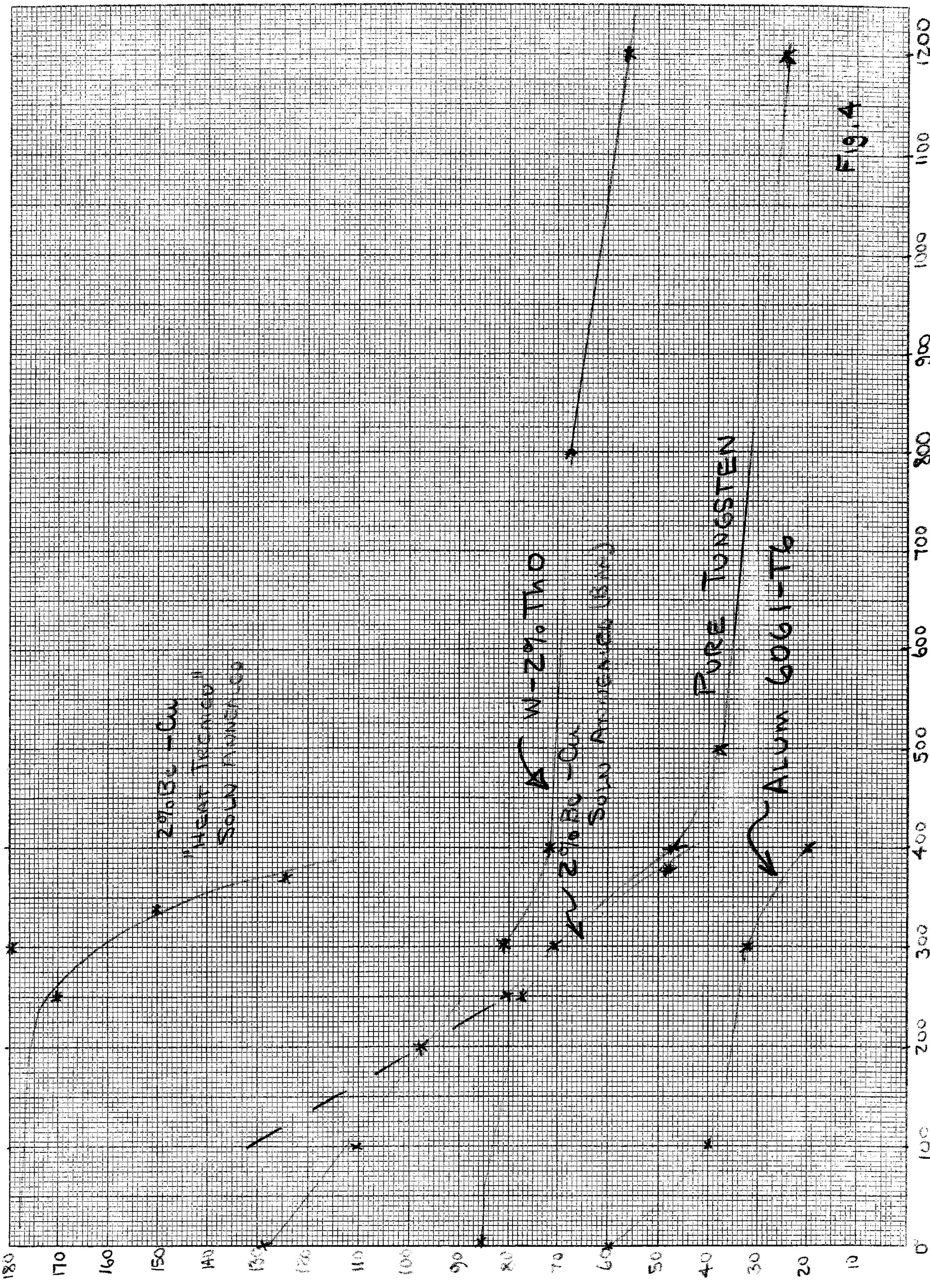

Ultimate Tensile Strength (kpsi)

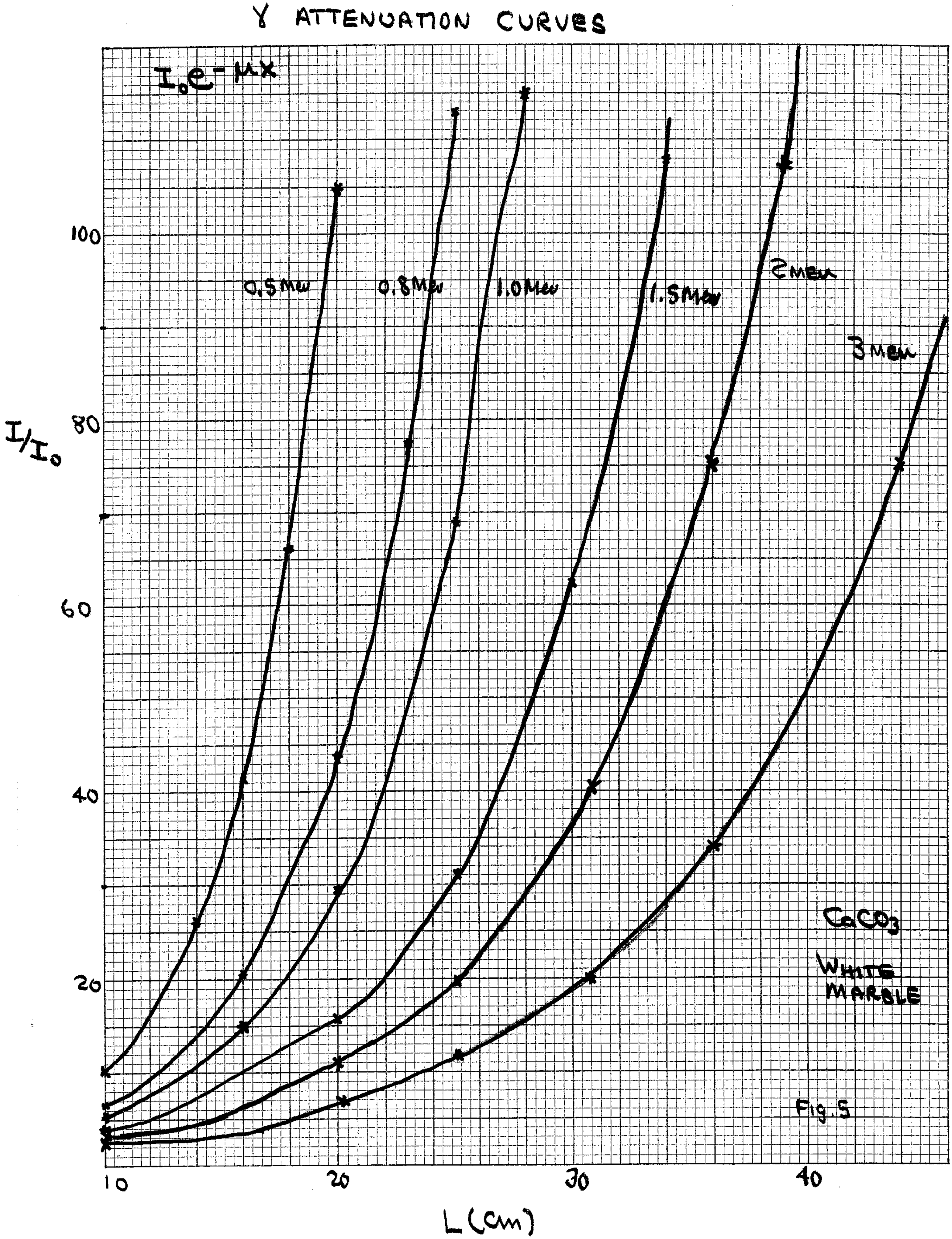
γ ATTENUATION CURVES
$I_0 e^{-\mu x}$
0.5 Mev
0.8 Mev
1.0 Mev
1.5 Mev
2 Mev
3 Mev
$CaCO_3$
WHITE MARBLE
I/I₀
100
80
60
40
20
10
20
30
40
L (cm)

Fig. 5

H_1, H_2 SWEEPING MAGNETS

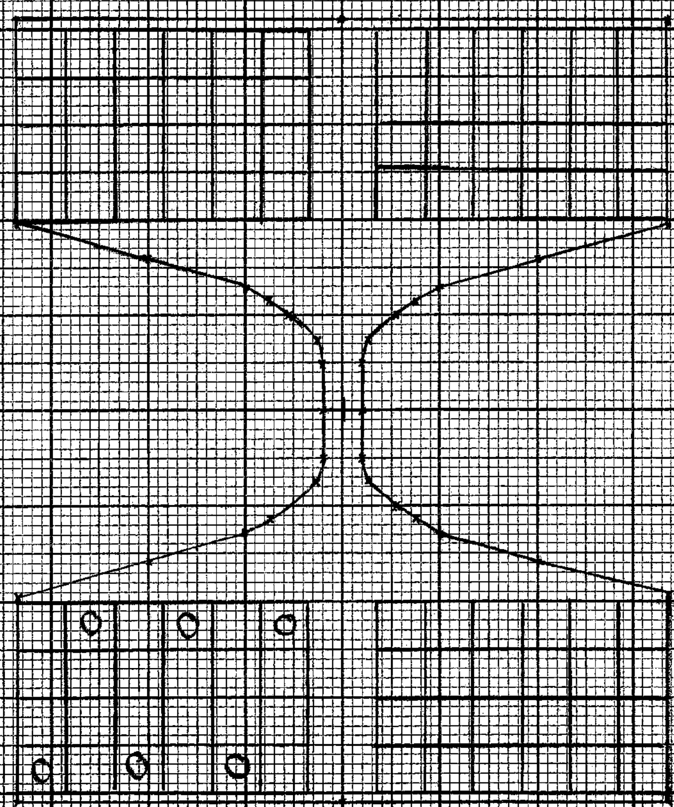

SCALE: 1/2

SECTION VIEW

Fig. 6

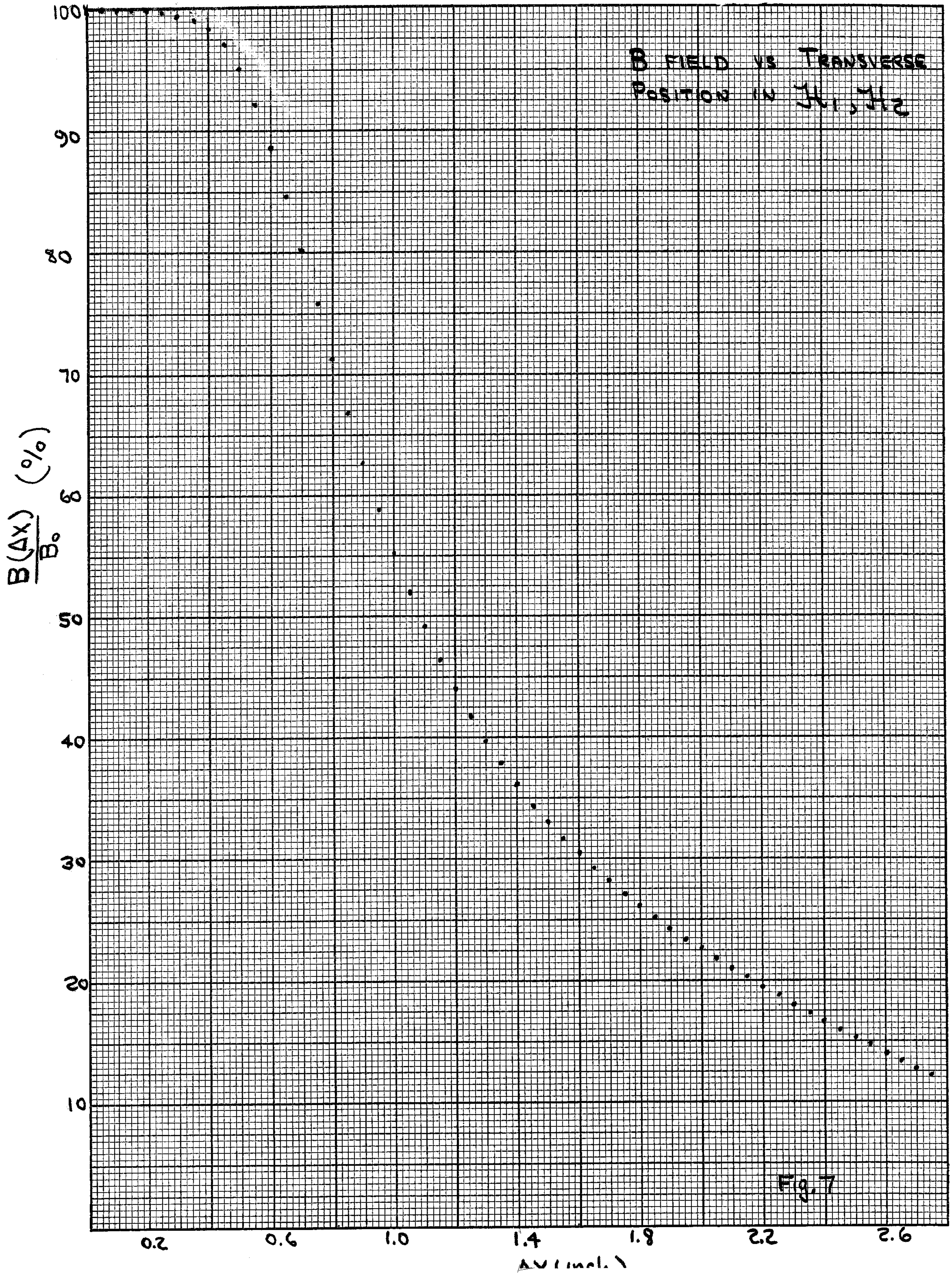
B FIELD VS TRANSVERSE POSITION IN H1, H2
B(Δx)/B₀ (%)
100
90
80
70
60
50
40
30
20
10
0.2
0.6
1.0
1.4
1.8
2.2
2.6
Fig. 7

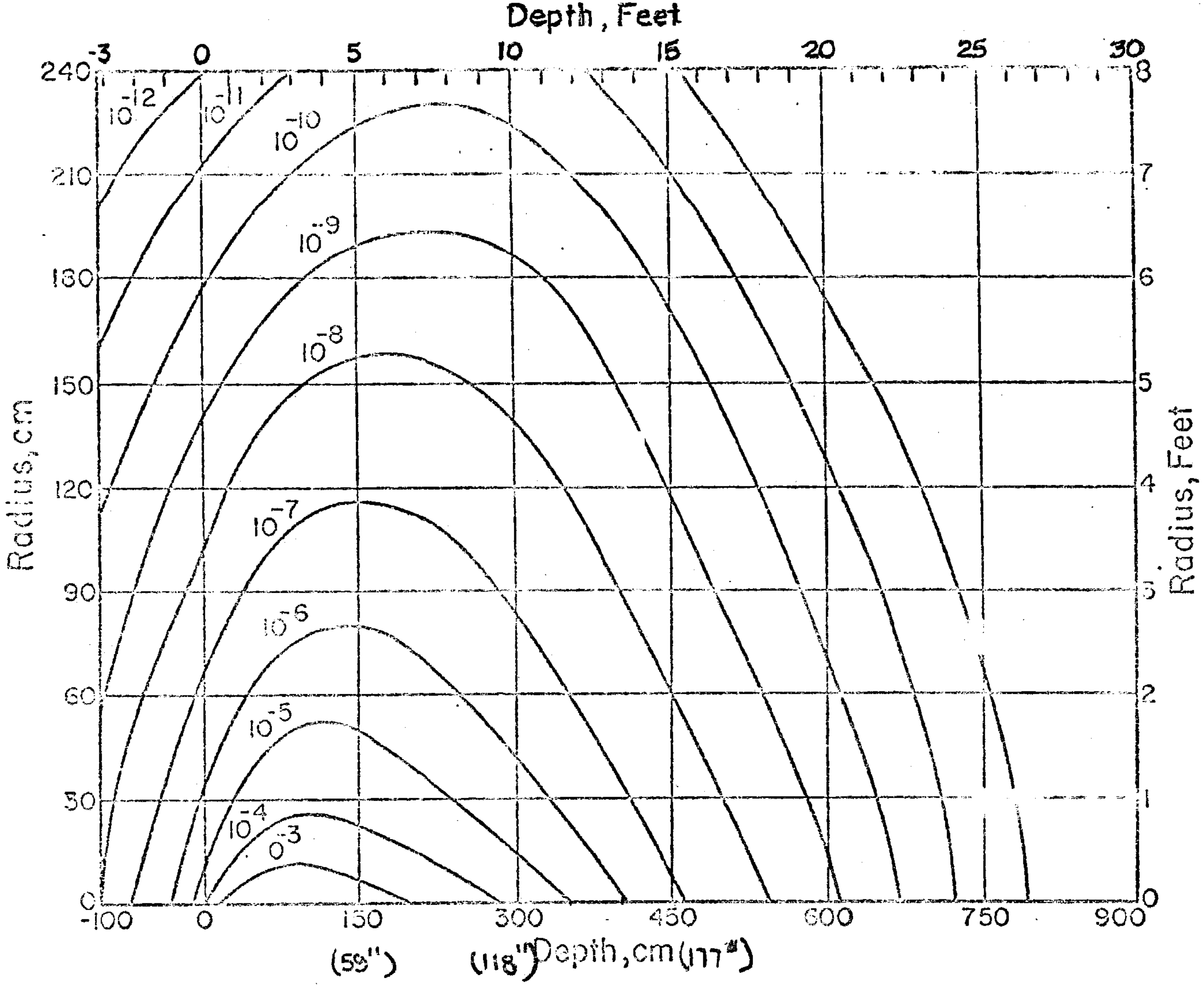

Fig. VIII. 3. 300 GeV/c protons incident on a solid iron cylinder. Contours of equal star density (stars/cm^3 & inc. proton). The beam of 0.3 x 0.3 cm cross section is centered on the cylinder axis and starts to interact at zero depth. The star density includes only those due to hadrons above 0.3 GeV/c momentum. Contours of higher star density are not shown for clarity of the plot, those of lower star density are not included due to statistical uncertainty.

400 GeV/c ~ 4/3 D

Fig. 8

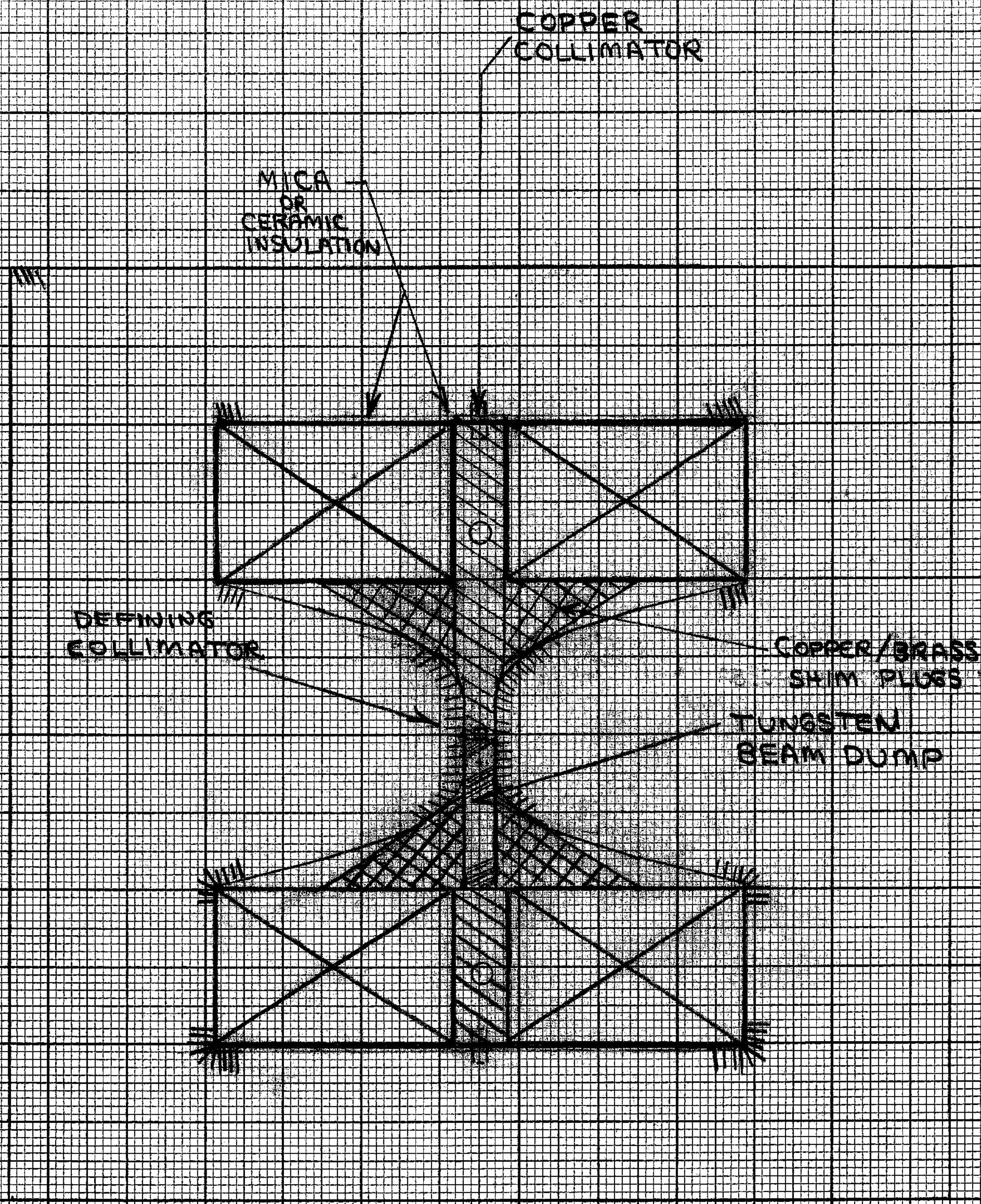

SECTION VIEW SCALE: 1/2

H_2 SWEEPING MAGNET, DEFINING COLLIMATOR, AND BEAM DUMP

Fig. 9

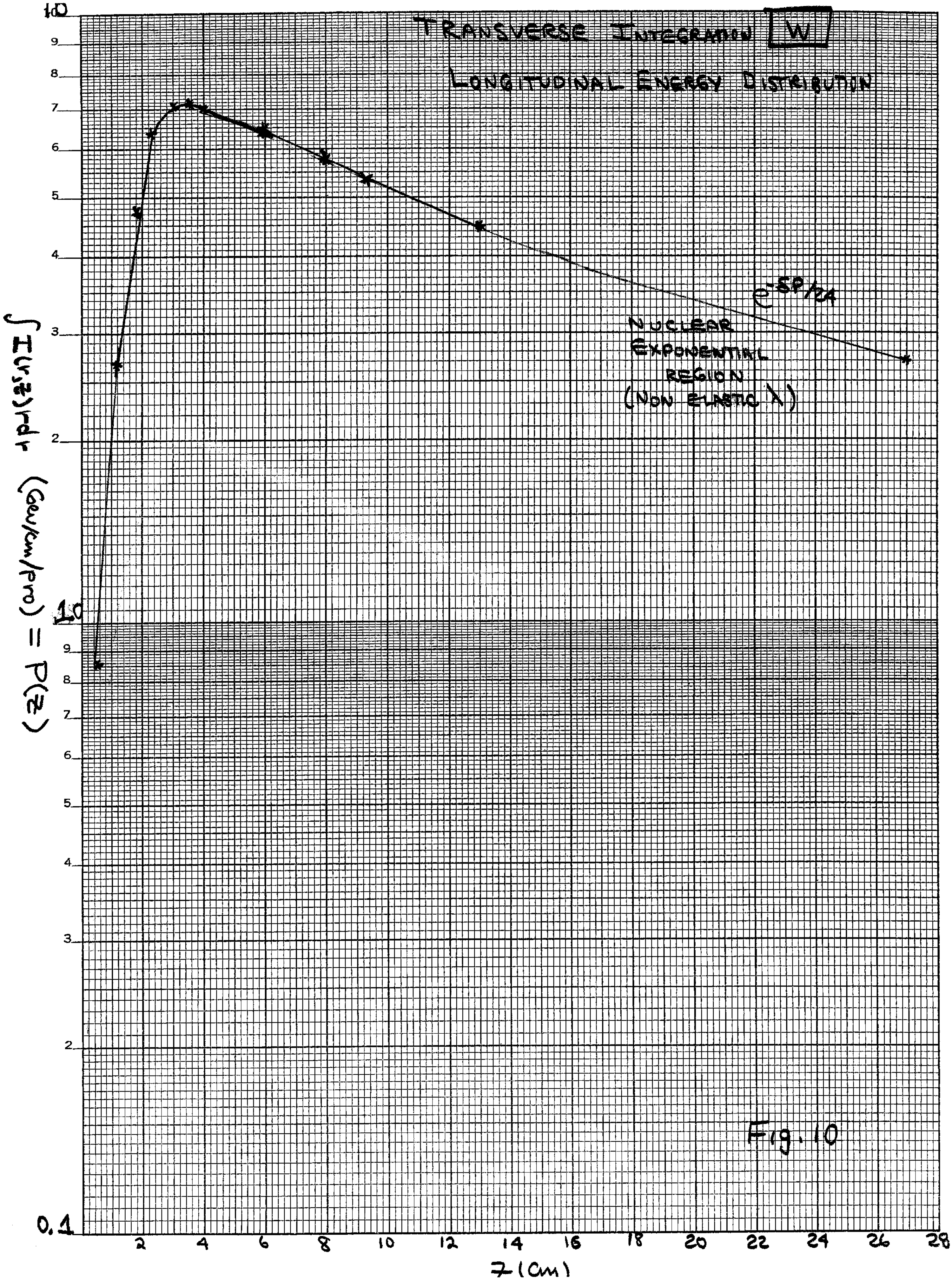
TRANSVERSE INTEGRATION W
LONGITUDINAL ENERGY DISTRIBUTION
$e^{-SP/24}$
NUCLEAR
EXPONENTIAL
REGION
(NON ELASTIC λ)
∫ I(r,z) r dr (z) = P(z) (GeV/cm/pro)
Z (cm)
10
9
8
7
6
5
4
3
2
1.0
0.1
2
4
6
8
10
12
14
16
18
20
22
24
26
28

Fig. 10

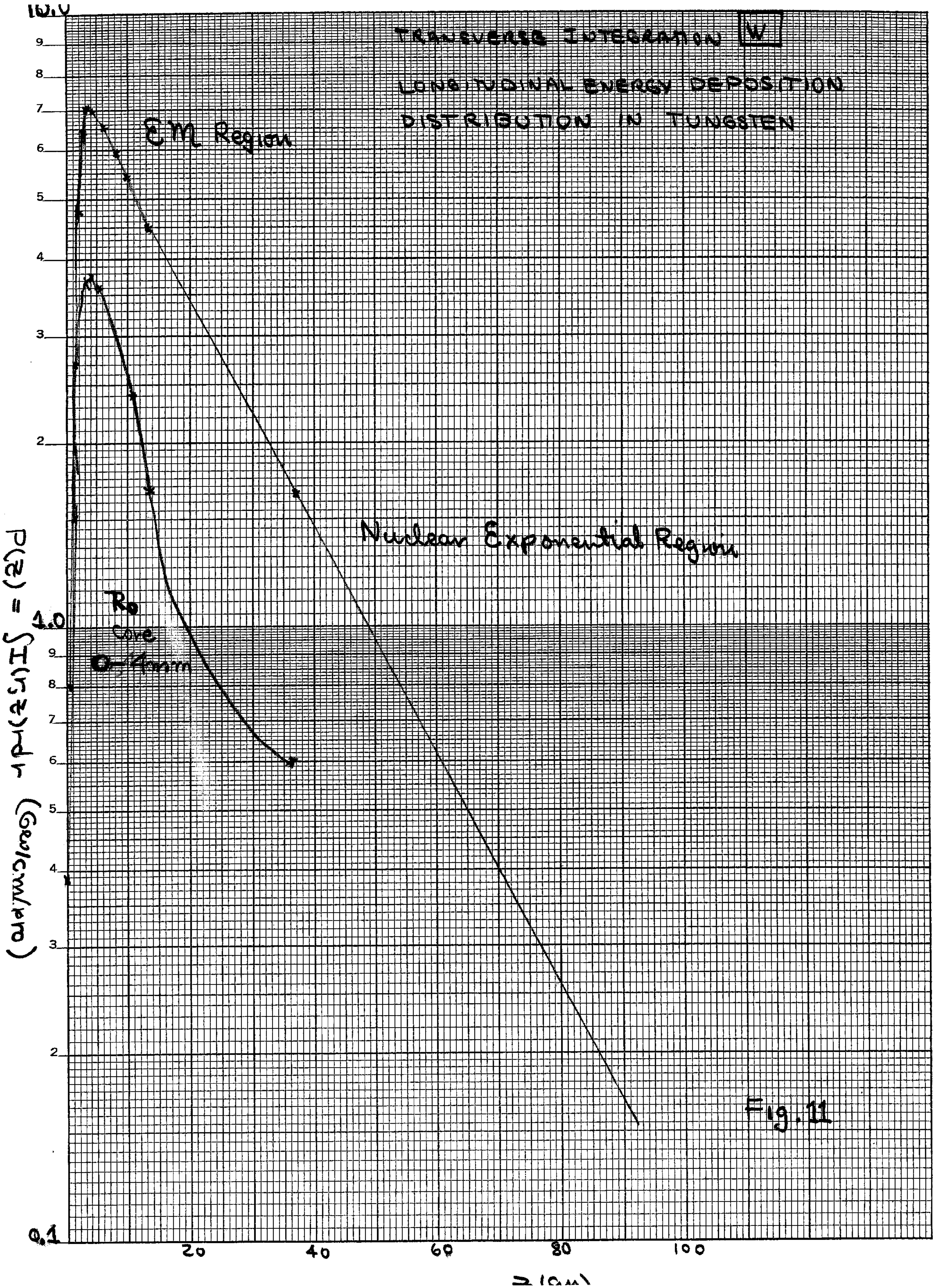
TRANSVERSE INTEGRATION W
LONGITUDINAL ENERGY DEPOSITION
DISTRIBUTION IN TUNGSTEN
EM Region
Nuclear Exponential Region
R₀ core 0-4mm
ρ(z) = ∫I(z,r)dr (GeV/cm/ep)
z (cm)
10.0
1.0
0.1
20
40
60
80
100

Fig. 11

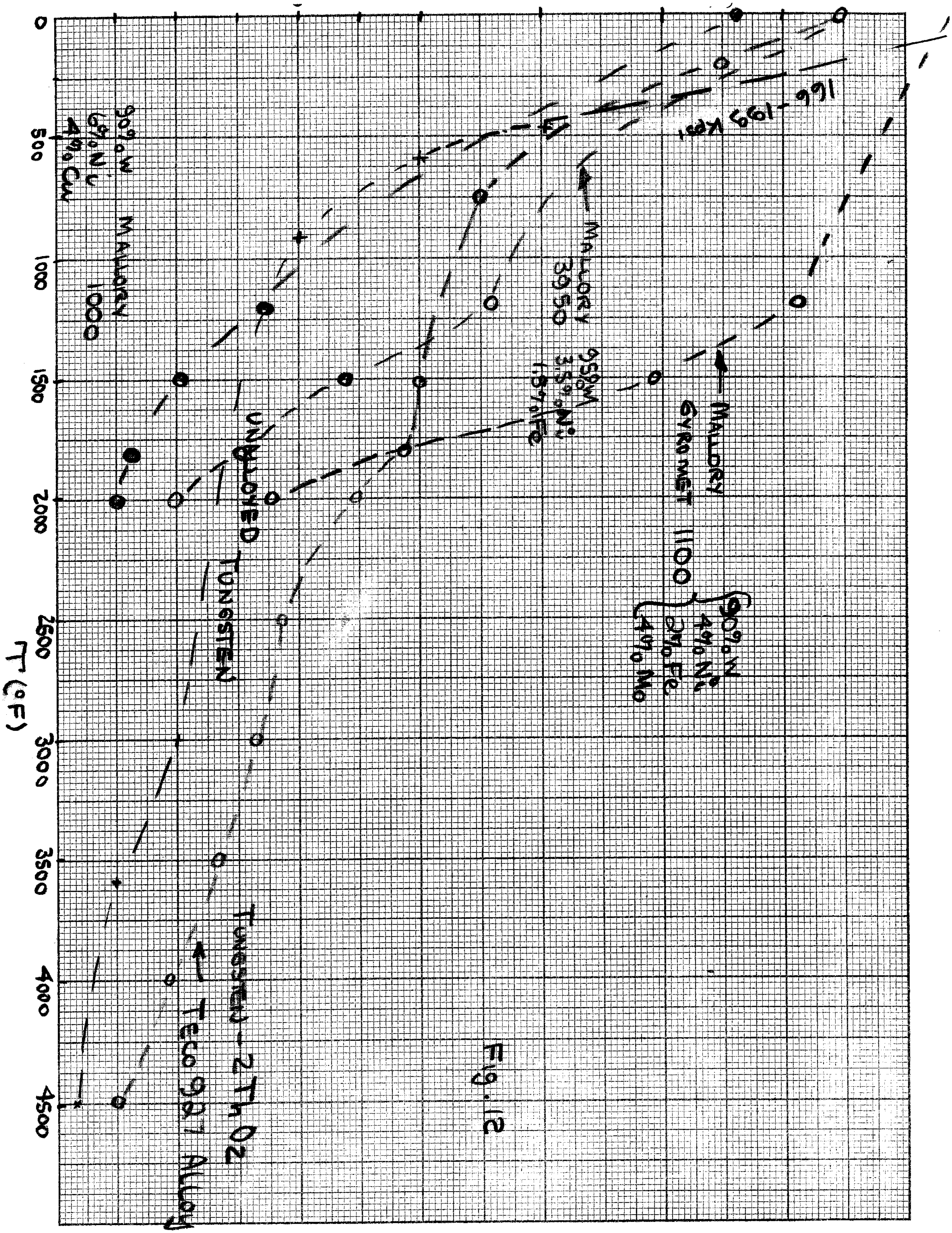
0
500
1000
1500
2000
2500
3000
3500
4000
4500
T (°F)
90% W
6% Ni
4% Cu
MALLORY
1000
MALLORY
3950
95% W
3.5% Ni
1.5% Fe
MALLORY
GYROMET 1100
90% W
4% Ni
2% Fe
4% Mo
UNALLOYED
TUNGSTEN
TUNGSTEN-2 ThO2
TECO 907 ALLOY
166-1993 KPSI

Fig. 12

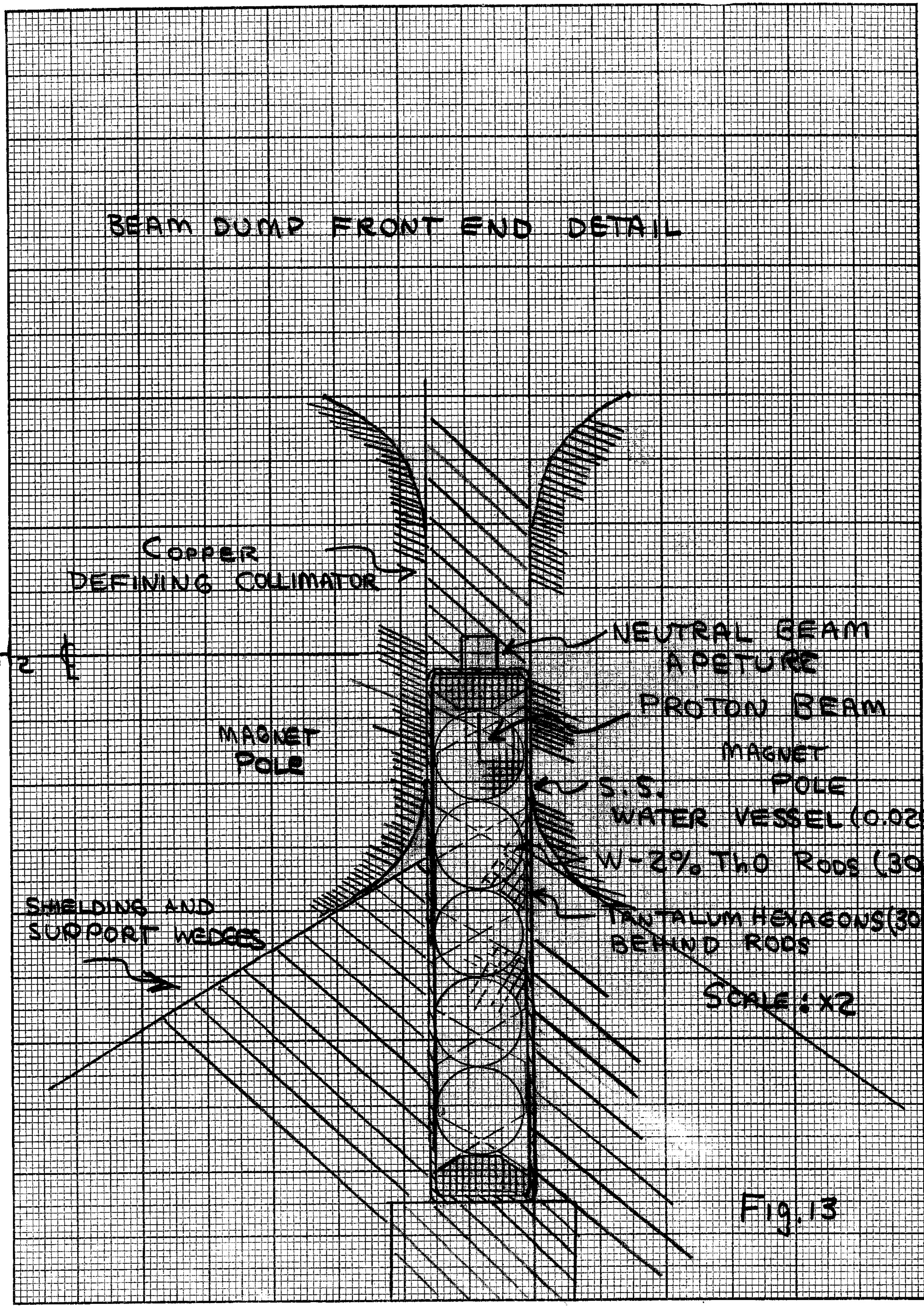
BEAM DUMP FRONT END DETAIL
COPPER
DEFINING COLLIMATOR
NEUTRAL BEAM
APETURE
PROTON BEAM
MAGNET
POLE
MAGNET
POLE
S.S.
WATER VESSEL (0.025")
W-2% ThO RODS (30cm
TANTALUM HEXAGONS (30cm)
BEHIND RODS
SHIELDING AND
SUPPORT WEDGES
SCALE: X2

Fig. 13

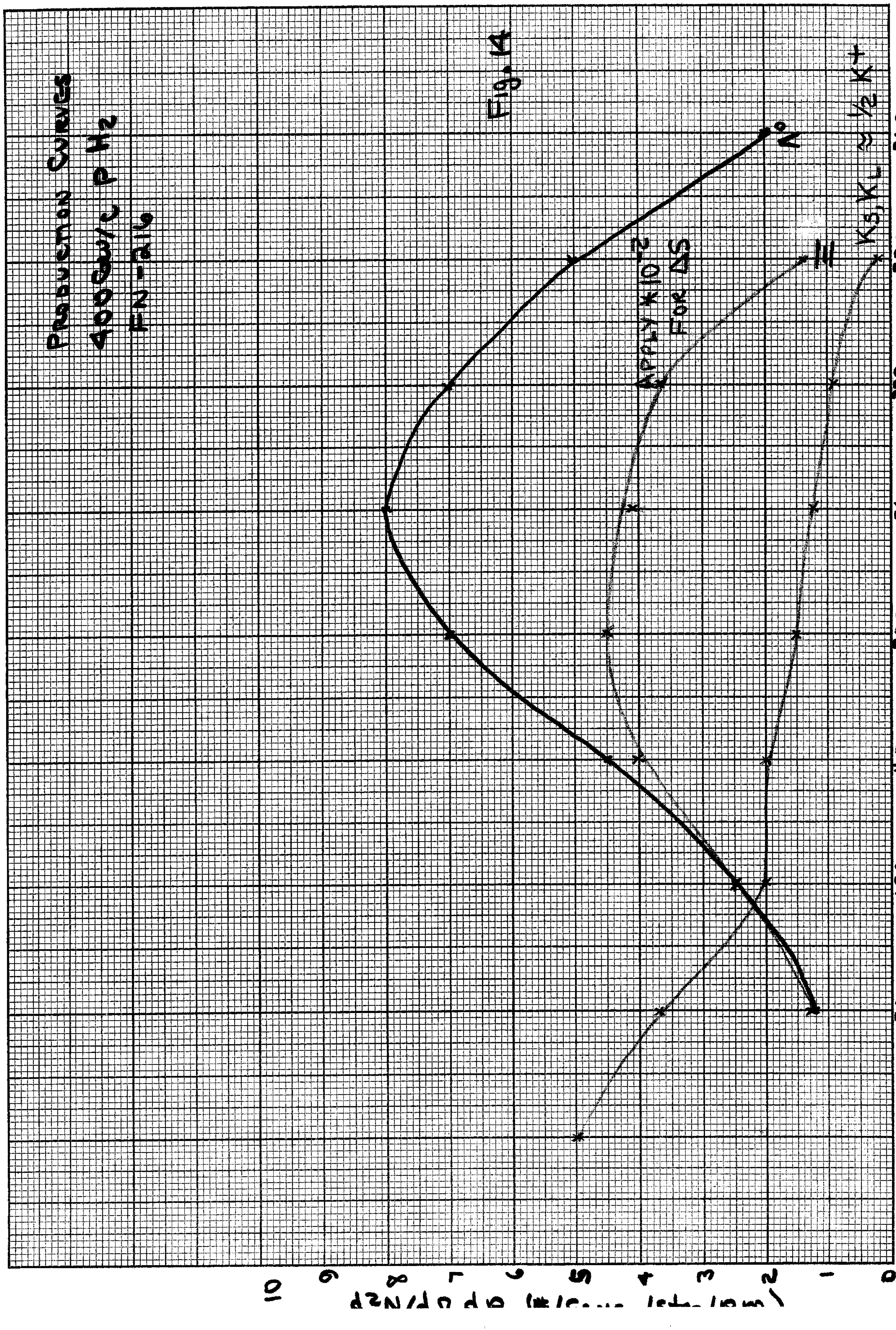
PRODUCTION CURVES
400 GeV/c P H2
FN-216
Fig. 14
APPLY * 10^-2
FOR ΔS
Λ°
Ξ
KS, KL ≈ 1/2 K+
40
80
120
160
200
240
280
320
360
0
1
2
3
4
5
6
7
8
9
10

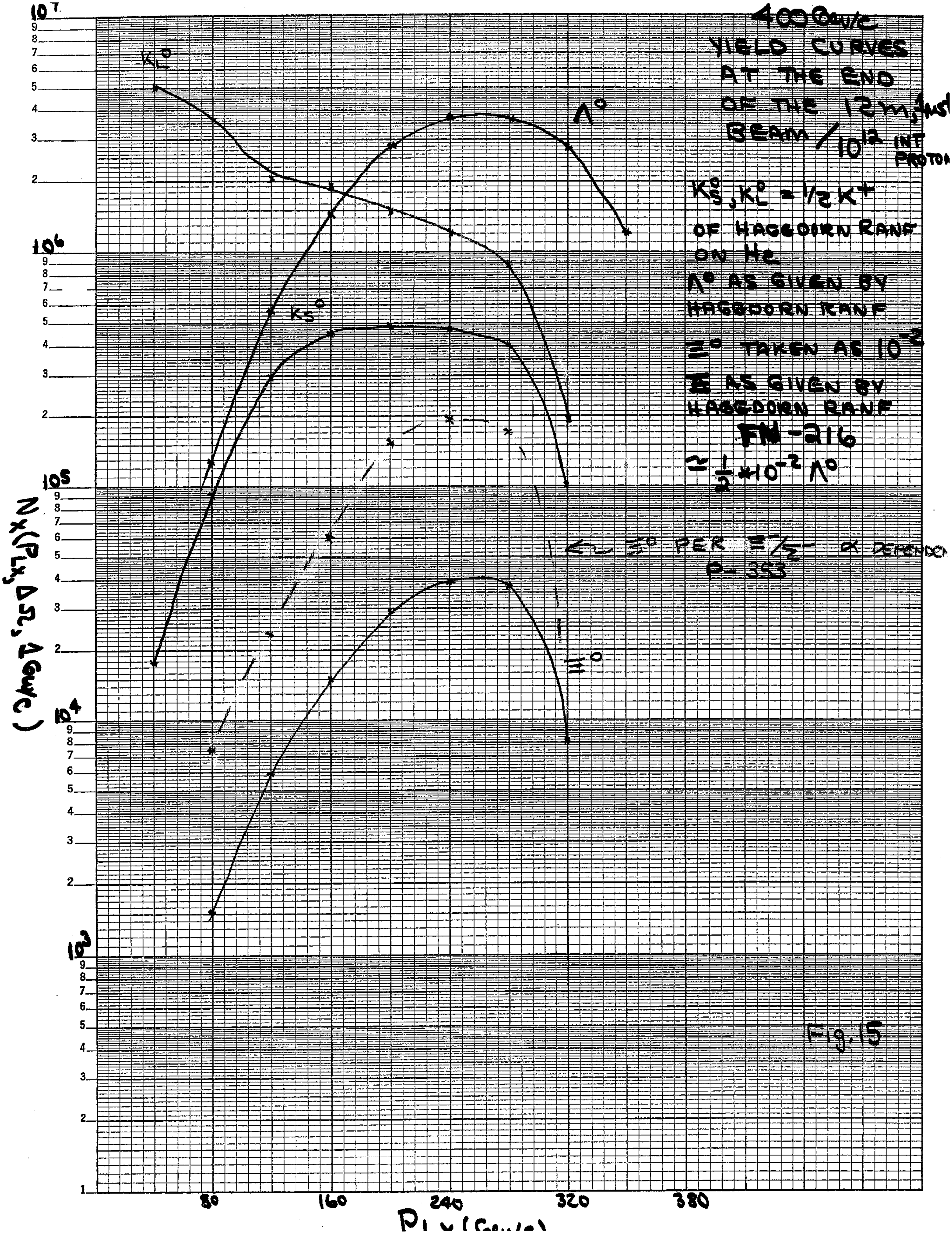
400 GeV/c
YIELD CURVES
AT THE END
OF THE 12 m, 1 msr
BEAM / 10^12 INT PROTONS
$K^0_S, K^0_L = 1/2 K^+$
OF HAGEDORN RANF
ON He
Λ^0 AS GIVEN BY
HAGEDORN RANF
Ξ^0 TAKEN AS 10^{-2}
Ξ AS GIVEN BY
HAGEDORN RANF
FN-216
$\simeq \frac{1}{2} \times 10^{-2} \Lambda^0$
Ξ^0 PER Ξ^-/Σ^- α DEPENDENCE
P-353
K_L^0
Λ^0
K_S^0
Ξ^0
$N_x(P_{Lx}, \Delta\Omega, \Delta GeV/c)$
P_{Lx} (GeV/c)
80
160
240
320
380

Fig. 15

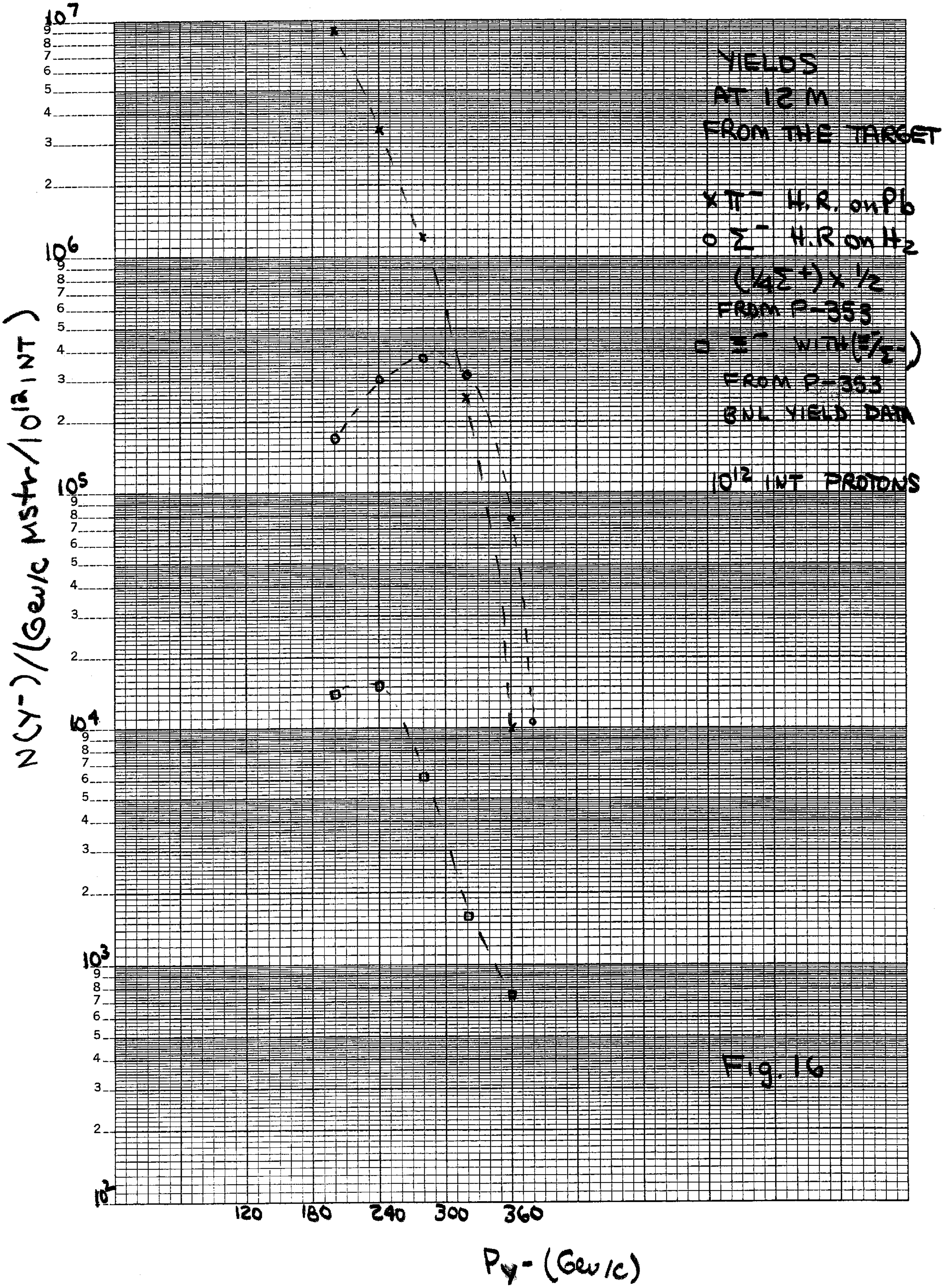
YIELDS
AT 12 M
FROM THE TARGET
× π⁻ H.R. on Pb
○ Σ⁻ H.R on H2
(1/4 Σ+) × 1/2
FROM P-353
□ Ξ⁻ WITH (Ξ/Σ-)
FROM P-353
BNL YIELD DATA
10^12 INT PROTONS
N(Y⁻)/(GeV/c Mstr/10^12 INT)
Py - (GeV/c)
120
180
240
300
360

Fig. 16

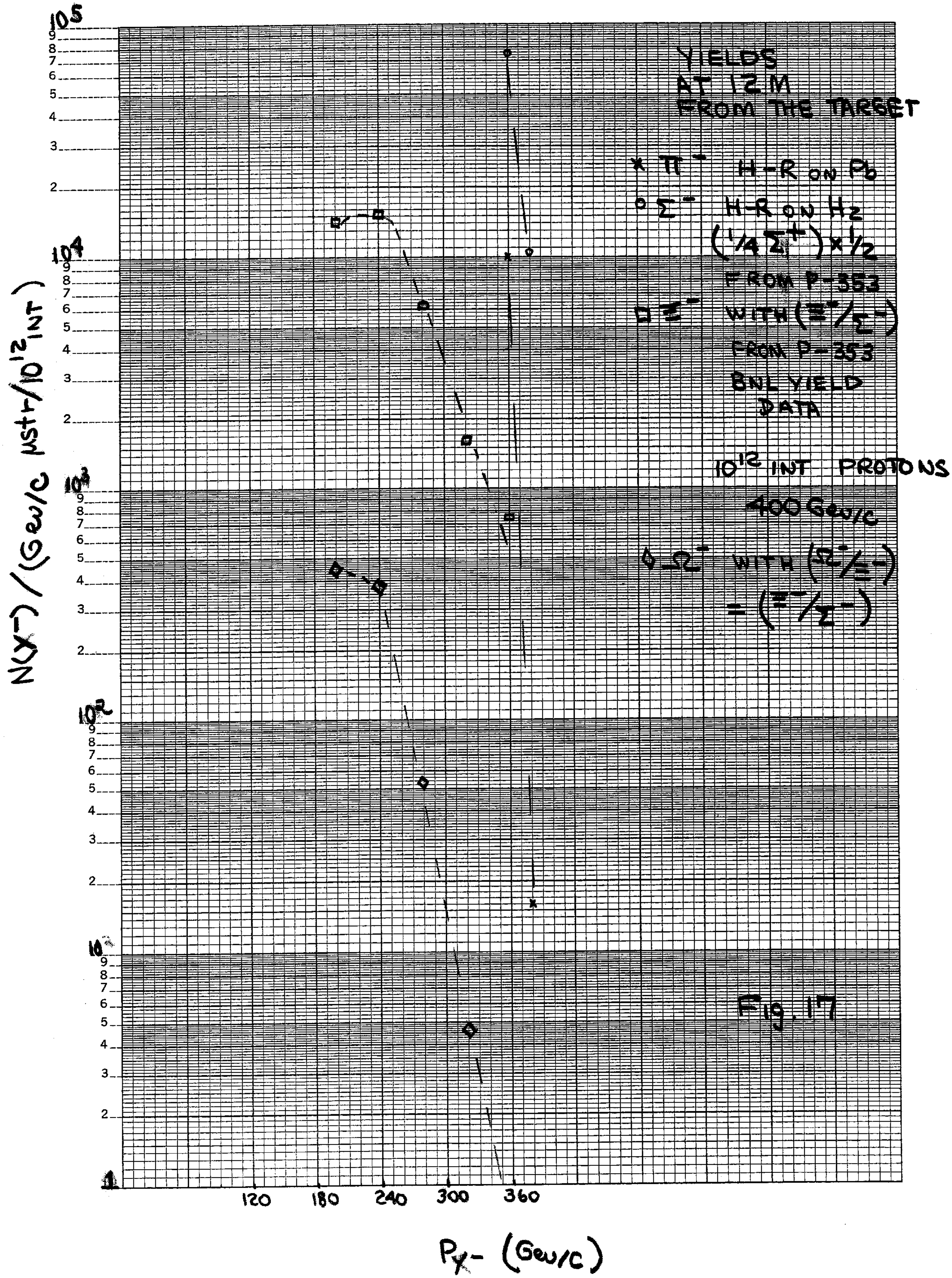
YIELDS
AT 12M
FROM THE TARGET
* π⁻ H-R ON Pb
○ Σ⁻ H-R ON H2
(1/4 Σ⁺) x 1/2
FROM P-353
□ Ξ⁻ WITH (Ξ⁻/Σ⁻)
FROM P-353
BNL YIELD
DATA
10¹² INT PROTONS
400 GeV/c
◇ Ω⁻ WITH (Ω⁻/Ξ⁻)
= (Ξ⁻/Σ⁻)
Fig. 17
N(X⁻) / (GeV/c μstr/10¹² INT)
Px- (GeV/c)
120
180
240
300
360
10⁵
10⁴
10³
10²
10
1